Target-oriented elastic full-waveform inversion through extended-migration redatuming

Ettore Biondi, Biondo Biondi, and Guillaume Barnier

ABSTRACT

The high computational cost of elastic full-waveform inversion (FWI) limits its applicability to real exploration datasets. We propose a target-oriented approach that alleviates the computational burden associated with elastic FWI by limiting the inversion process to only a portion of the subsurface where an accurate and high resolution elastic model is needed (e.g., reservoir level). The proposed method is based on the reconstruction of the data generated within the target area at a depth level directly above it. This data reconstruction is performed by an extended least-squares migration of the surface data followed by a demigration to the desired depth level. We demonstrate the efficacy of this approach on a layered model in which a complex reflector is considered to be our inversion target and only pressure data are recorded.

INTRODUCTION

FWI uses all the frequency information contained in the observed data; hence, it has the ability to simultaneously recover both the long- and short-wavelength components of the subsurface structures (Tarantola, 1984; Virieux and Operto, 2009). Moreover, since it is based on the solutions of any wave equation, it can correctly account for all the non-linear effects present in seismic data (e.g., multiple scattering and multipathing). Despite the recent hardware advancements in computational technologies, on exploration datasets only acoustic or pseudo-acoustic FWI algorithms are commonly applied (Sirgue et al., 2010). This trend is due to the fact that the computational cost of elastic FWI is much higher compared to the acoustic counter part (Fichtner, 2010). However, acoustic approximations incorrectly model the elastic amplitude responses and possibly provide incorrect inverted elastic parameters unless specific objective functions are employed (Bozdağ et al., 2011). If a ray-approximation is considered, amplitude-versus-offset (AVO) or -angle (AVA) techniques can be used to invert the elastic parameters of the subsurface reflectors (Yilmaz, 2001). Despite their low computational cost, these methods are limited to simple geological scenario and can correctly retrieve only the low resolution component of complex interfaces.

Different methods have been proposed to diminish the computational intensity of the elastic FWI process. Some of these algorithms are based on acoustic approximations in which the amplitudes are corrected to mimic the elastic effects that otherwise

would be neglected (Veitch et al., 2012; Hobro et al., 2014). Agudo et al. (2016) proposed a method in which a matching filter is used to mitigate the elastic effects present in the observed data and then an acoustic FWI algorithm is applied. The filtering and inversion process are performed iteratively until convergence is reached. A different approach is to reconstruct the data that would have been recorded if the acquisition geometry was sunk in the subsurface (Claerbout and Doherty, 1972; Wapenaar et al., 1992). In this case, by assuming an approximately correct propagation wave speed of the overburden, it is possible to move the sources and receivers to different positions compared to the real ones. This procedure is commonly referred to as redatuming. After this step, the reconstructed data can be used to apply imaging or inversion procedures where the model above the redatuming level is completely neglected (Bevc, 1997).

The proposed algorithm follows a redatuming approach. In fact, in most real applications, high resolution elastic property models are only necessary within limited portions of the entire subsurface (e.g., within the reservoirs). With this concept in mind, we propose a target-oriented elastic FWI approach where localized elastic data are reconstructed within the area of interest using an extended acoustic least-squares migration step and then elastically inverted. The data reconstruction enables us to limit the computational domain to only the area of interest. In order to perform the acoustic least-squares migration we assume that a relatively correct and smooth compressional wave speed model is known. The goal of the acoustic extended migration is to map the elastic data difference between the observed pressure and the one generated by the initial elastic model into a localized area of interest of the subsurface. In this operation we assume that most of the energy in the data difference is generated within the target inversion area. The extension of the scattering condition enables us to fully capture the kinematics and amplitudes of all the events present in the data difference. In fact, elastic effects and multiple scattering occurring within the target area can be modeled by the inverted extended perturbation. In our application we use a subsurface-offset Born extended modeling operator (Prucha et al., 1999; Sava and Fomel, 2003). After performing this migration procedure, we model the background elastic data only within the area of interest and add to them the demigrated data constructed using the inverted extended perturbation. The reconstructed data are comparable to the one that would have been recorded if the propagations were occurring only within the true target portion of the subsurface. Therefore, these data can be used to perform an elastic FWI to obtain the high-resolution model within the target area.

We test our proposed approach on a synthetic 2D example where pressure data are recorded from a layered model in which the deepest reflector is considered to be the inversion target. First, we compare the reconstructed data with the true pressure generated by only the area of interest using a sunk acquisition geometry. Then, we assess the agreement between the elastic FWI results obtain with the true localized data and the one reconstructed using the proposed method.

THEORY

Commonly, the FWI problem is defined by the following misfit function:

$$\phi_{FWI}(\mathbf{m}) = \frac{1}{2}\left\|\mathbf{f}(\mathbf{m}) - \mathbf{d}_{obs}\right\|_2^2 \tag{1}$$

that is usually minimized using a gradient-based method to seek the subsurface model $\mathbf{m}$ that matches the observed data $\mathbf{d}_{obs}$ using the non-linear wave-equation modeling operator $\mathbf{f}$. In most seismic application, the vector $\mathbf{d}_{obs}$ represents the recorded pressure and particle velocities or displacements at the receiver locations. Here we only consider pressure data and assume that a true Earth model $\mathbf{m}_{true}$ generated the observed recordings. Therefore, the observed data are given by $\mathbf{d}_{obs} = \mathbf{f}(\mathbf{m}_{true})$.

The minimization of the objective function in equation 1 starts by choosing an initial subsurface model $\mathbf{m}_0$. In this discussion we assume that the model difference $\Delta\mathbf{m} = \mathbf{m}_{true} - \mathbf{m}_0$ is localized within a limited portion of the subsurface. Therefore, most of the energy contained in the initial data residuals ($\Delta\mathbf{d} = \mathbf{f}(\mathbf{m}_0) - \mathbf{f}(\mathbf{m}_{true})$) is generated within that limited portion of the subsurface. Ideally, we would like to avoid propagating through the correct overburden and limit our computational domain to the target area. One possible solution is to reconstruct the data that would have been observed if the acquisition geometry was sunk at the top of the target area and the propagation was only occurring within that portion; hence, the overburden is completely ignored. The data difference recorded by this sunk geometry can be written as follows:

$$\Delta\mathbf{d}' = \mathbf{f}'(\mathbf{K}\mathbf{m}_0) - \mathbf{f}'(\mathbf{K}\mathbf{m}_{true}), \tag{2}$$

where $\mathbf{K}$ is an operator that restricts the model to only the target area. Hereinafter, the symbol $'$ denotes quantities related to the sunk geometry and the target subsurface portion. If the surface and the sunk acquisition geometries illuminate the target area identically, the least-squares migration process applied to the respective data residuals ($\Delta\mathbf{d}$ and $\Delta\mathbf{d}'$) produces the same inverted extended perturbation. Mathematically, this observation can be expressed by the following:

$$\Delta\tilde{\mathbf{m}} = \mathbf{K}\left[\tilde{\mathbf{B}}^*\tilde{\mathbf{B}}\right]^{-1}\tilde{\mathbf{B}}^*\Delta\mathbf{d} = \left[\tilde{\mathbf{B}}'^*\tilde{\mathbf{B}}'\right]^{-1}\tilde{\mathbf{B}}'^*\Delta\mathbf{d}', \tag{3}$$

where $\Delta\tilde{\mathbf{m}}$ is the inverted extended perturbation, $\tilde{\mathbf{B}}$ and $\tilde{\mathbf{B}}'$ are the extended Born modeling operators for the surface and sunk acquisition geometries, respectively, and the symbol $*$ denotes the adjoint of an operator. Additionally, to fully reconstruct the data within the target area the following condition must be satisfied:

$$\Delta\mathbf{d}' = \tilde{\mathbf{B}}'\Delta\tilde{\mathbf{m}}. \tag{4}$$

If these conditions are met, then after performing a least-squares migration of the surface data difference $\Delta\mathbf{d}$, we are able to reconstruct the sunk-acquisition data difference through equation 4. With this term we can thus obtain the data coming from the target area by reordering the terms in equation 2.

NUMERICAL EXAMPLE

In the synthetic application described here we use an elastic isotropic wave-equation operator and employ an acoustic extended Born modeling operator for the data reconstruction step since we are interested in inverting the compressional wave events (or *PP* events) recorded at the surface.

The three panels of Figure 1 show the true P- and S-wave velocities, and density model, respectively. This subsurface model is composed of four interfaces in which last one presents a sinusoidal shape such that the Zoeppritz's equations cannot correctly predict the reflection coefficient since the planar reflection assumption is not valid (Aki and Richards, 2002). Therefore, conventional amplitude-versus-offset (AVO) inversion algorithms would not be able to correctly retrieve the elastic parameter contrasts.

Using a finite-difference operator based on the velocity-stress formulation of the elastic isotropic wave equation (Virieux, 1986), we model the pressure field recorded by 1001 receivers and 101 explosive sources evenly sampled by 10 and 100 meters at $z = 0$ km, respectively. We inject a broadband wavelet with frequency content between 2 and 30 Hz. Figure 2 displays a representative shot gather for the source placed at $x = 5$ km. In the recorded pressure four *PP* reflections can be clearly distinguished as well as the direct arrival. Moreover, multiple scattering effects are noticeable in the last of these four events. The initial elastic model is generated by applying a strong smoothing operator to all the last-reflector elastic parameters of the true model. Figure 3 shows the initial P-wave velocity model in which the deepest complex interface is now almost planar. In fact, most of the energy observed in the initial data residuals (i.e., $\Delta\mathbf{d}$) is localized within the last reflected event. Using the surface data residuals and the P-wave initial velocity model of Figure 3, we perform a least-squares acoustic extended migration by solving iteratively the inverse system shown in equation 3 using 50 iterations of a linear-conjugate gradient approach (Aster et al., 2005). During the inversion a model-space weighting operator is used to limit the perturbation to the target area. We also perform the same migration process using the sunk-acquisition residuals to verify the equality condition described by the same equation. In this application we limit the target area between 1.2 and 2 km depth. Figure 4 displays the zero-lag offset sections after the inversion process using the two different acquisitions. Both surface and sunk acquisitions provide a similar migrated section. We notice that a broader illumination is observed when the sunk-acquisition residuals are migrated (Figure 4b). If we analyze the behavior of a representative common image gather (CIG) extracted at $x = 5$ km for both acquisitions, we observe a similar amplitude response along with some inversion truncation artifacts (Figure 5).

The ultimate goal is to reconstruct the true sunk-acquisition data (equation 2) through this extended migration process (equation 4). Figure 6 shows the comparison between the true sunk-acquisition residuals and the reconstructed one. Apart from some linear-moveout artifacts, the data reconstructed residuals closely match the true one. Additionally, since the two acquisitions do not present the same illumination pattern, the far-offset traces are not perfectly reproduced. In the next step, we

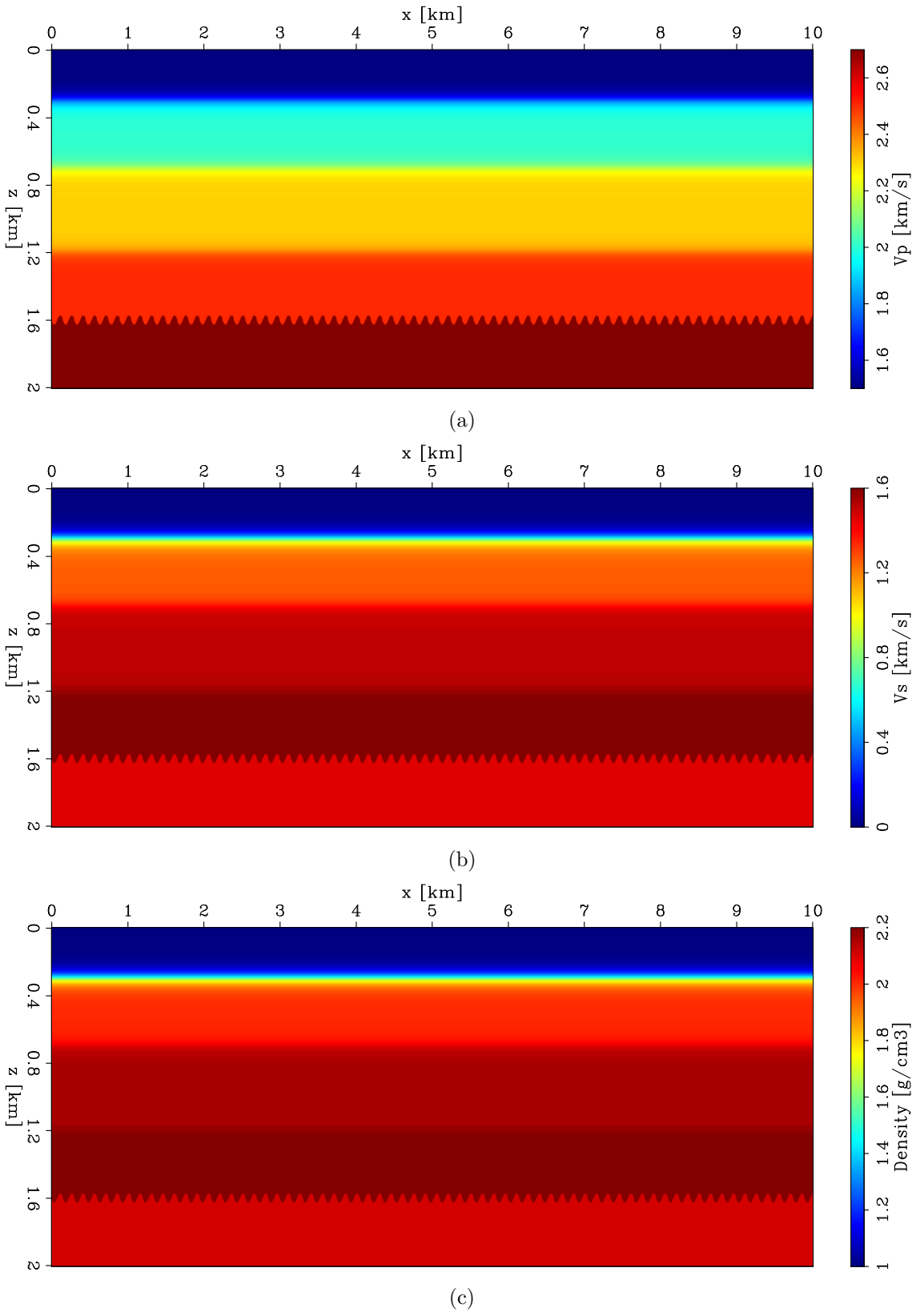

Figure 1: True elastic subsurface model used in the described numerical example. (a) P-wave velocity, (b) S-wave velocity, and (c) density model. [**ER**]

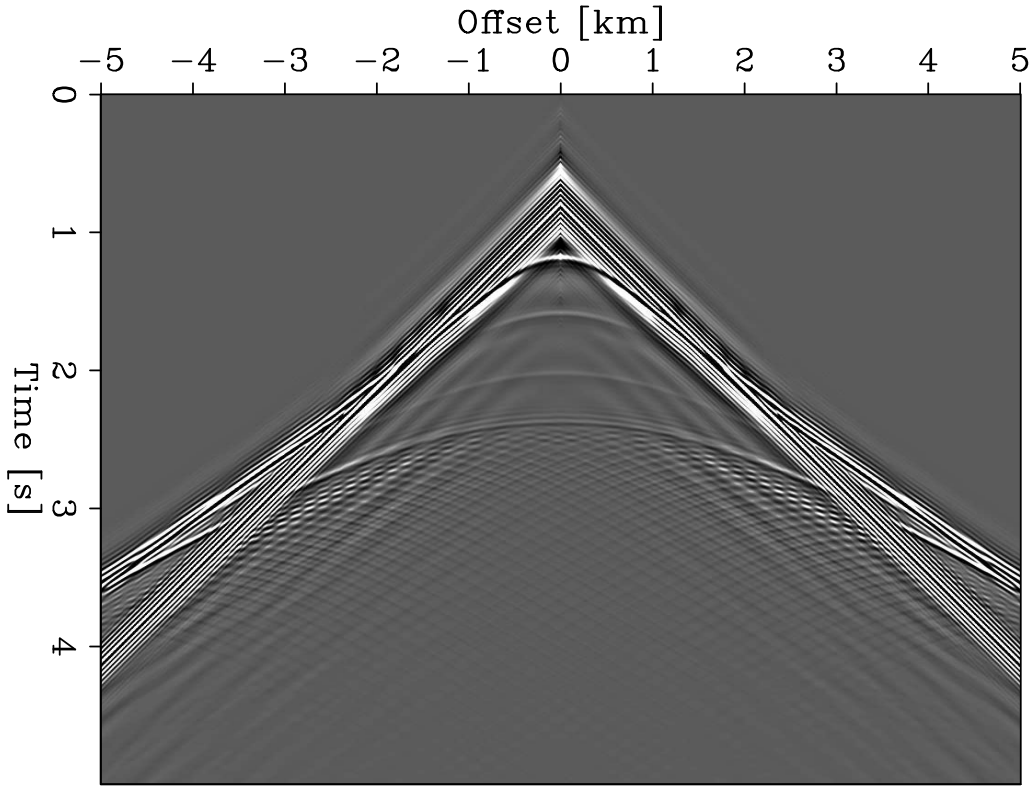

Figure 2: Pressure shot gather for a source placed at $z = 0$ km and $x = 5$ km and receivers evenly spaced at the surface of the elastic model shown in Figure 1. [**CR**]

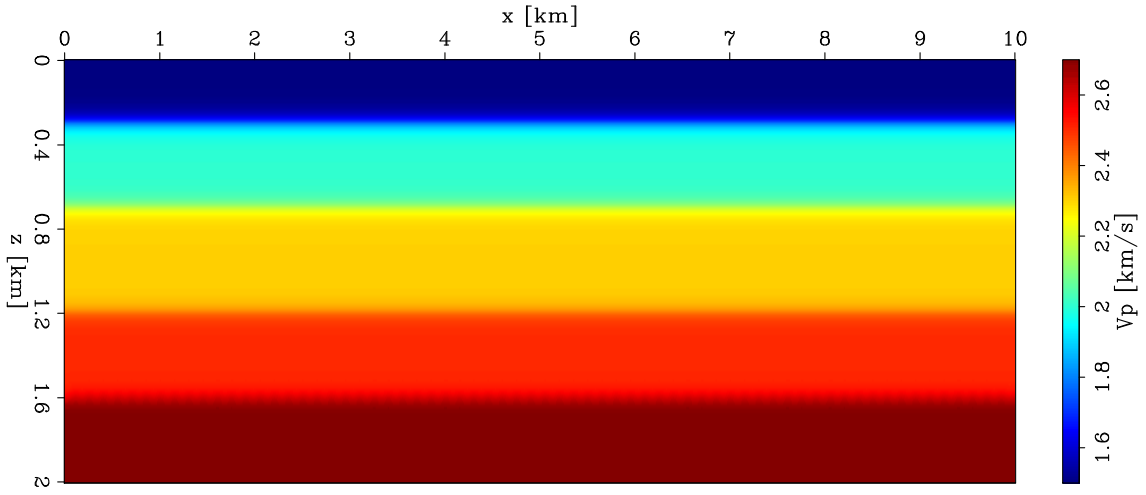

Figure 3: P-wave velocity model used for performing the least-squares migration process in which a smoothing operator is applied to the last sinusoidal reflector. The same smoothing operator has been applied to other model parameters to generate the initial elastic predicted pressure. [**ER**]

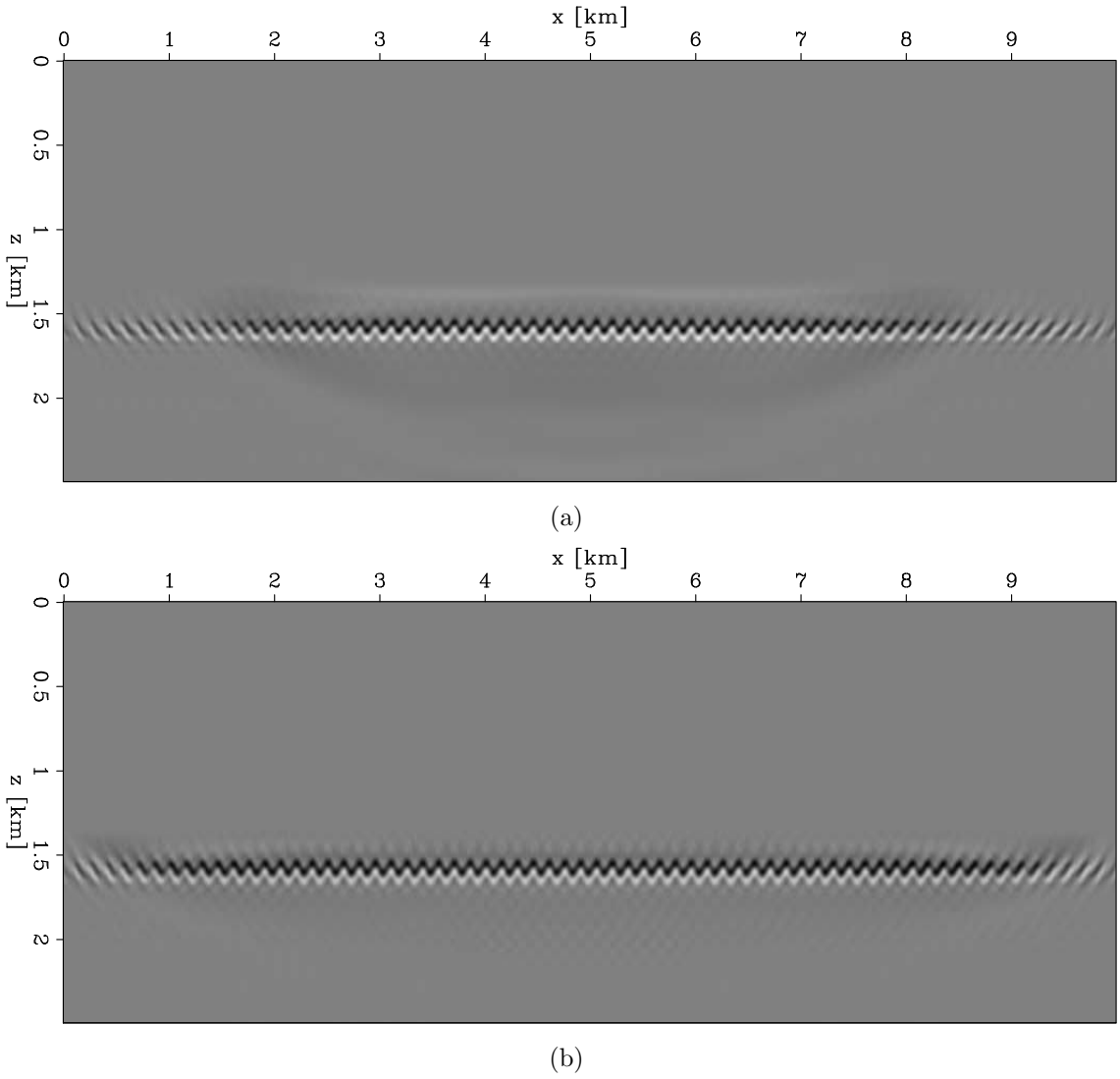

Figure 4: Inverted zero-offset section obtained after a 70 iterations of a linear conjugate-gradient algorithm using (a) the surface $\Delta\mathbf{d}$ and (b) sunk-acquisition data difference $\Delta\mathbf{d}'$. [**CR**]

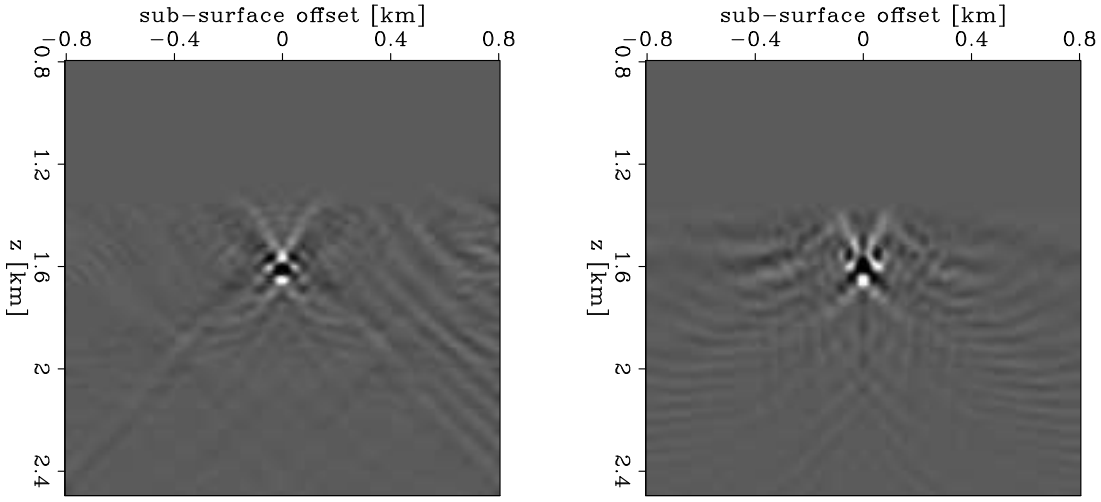

Figure 5: CIGs at $x = 5$ km for (a) surface and (b) sunk-acquisition data difference. A model-space weighting operator has been used to limit the extended perturbation to be within the target area. [**CR**]

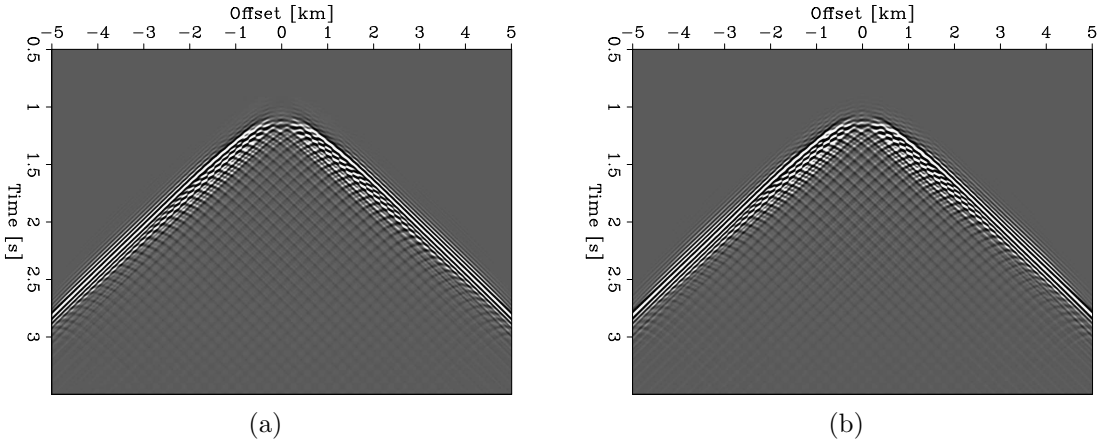

Figure 6: Comparison between (a) true sunk-acquisition data difference (equation 2) and (b) the reconstructed one (equation 4). [**CR**]

minimize the objective function in equation 1 related to the localized elastic FWI problem using a multiscale approach (Bunks et al., 1995). We parameterize this objective function in terms of P- and S-wave velocities, and density. We invert three consecutive bands, namely 2-10, 2-20, and 2-30 Hz, by applying 50 iterations of a non-linear conjugate-gradient algorithm for each one of them. During the inversion we constrain the acquisition geometry between 2 and 8 km to limit the effect of the different illumination mentioned before.

The inverted model parameters when the true sunk-acquisition data are used are shown in Figure 7. The shape and amplitude of the missing perturbations from the initial model are correctly retrieved for all model parameters. Figure 8 shows the same inverted model when the reconstructed data are used during the inversion. Both figures present the same color ranges. The inverted wave-velocity parameters are similar to the ones retrieved when the true sunk data are used. The artifacts present in these parameters are due to the truncation error made during the migration process as well as the slightly different illumination between the surface and sunk acquisitions. On the other hand, the inverted density is more affected by these reconstruction errors and the model matching is not as accurate compared to the two wave velocities. Finally, thanks to the restriction of the elastic FWI problem to only the last interface, and thus by completely neglecting the overburden, the computational cost is decreased by a factor of approximately five.

CONCLUSIONS

We present a target-oriented elastic FWI algorithm in which the events generated within a target area of the subsurface are reconstructed via an extended least-squares migration process. During this step, we assume an identical illumination between the surface and localized acquisitions and the capability of reconstructing the sunk-acquisition data difference by a demigration process of the inverted extended perturbation.

We show the efficacy of the proposed algorithm on a layered elastic model in which the inversion target is represented by a complex interface in the subsurface. In fact, despite some artifacts due to the truncation error during the migration process, the inverted parameters are close to the true ones. In addition, the targeting of the inversion to only the last interface significantly reduces the computational cost of the FWI problem.

REFERENCES

Agudo, O. C., N. da Silva, M. Warner, and J. Morgan, 2016, Acoustic full-waveform inversion in an elastic world: Presented at the 2016 SEG International Exposition and Annual Meeting.

Aki, K. and P. G. Richards, 2002, Quantitative seismology: University Science Books.

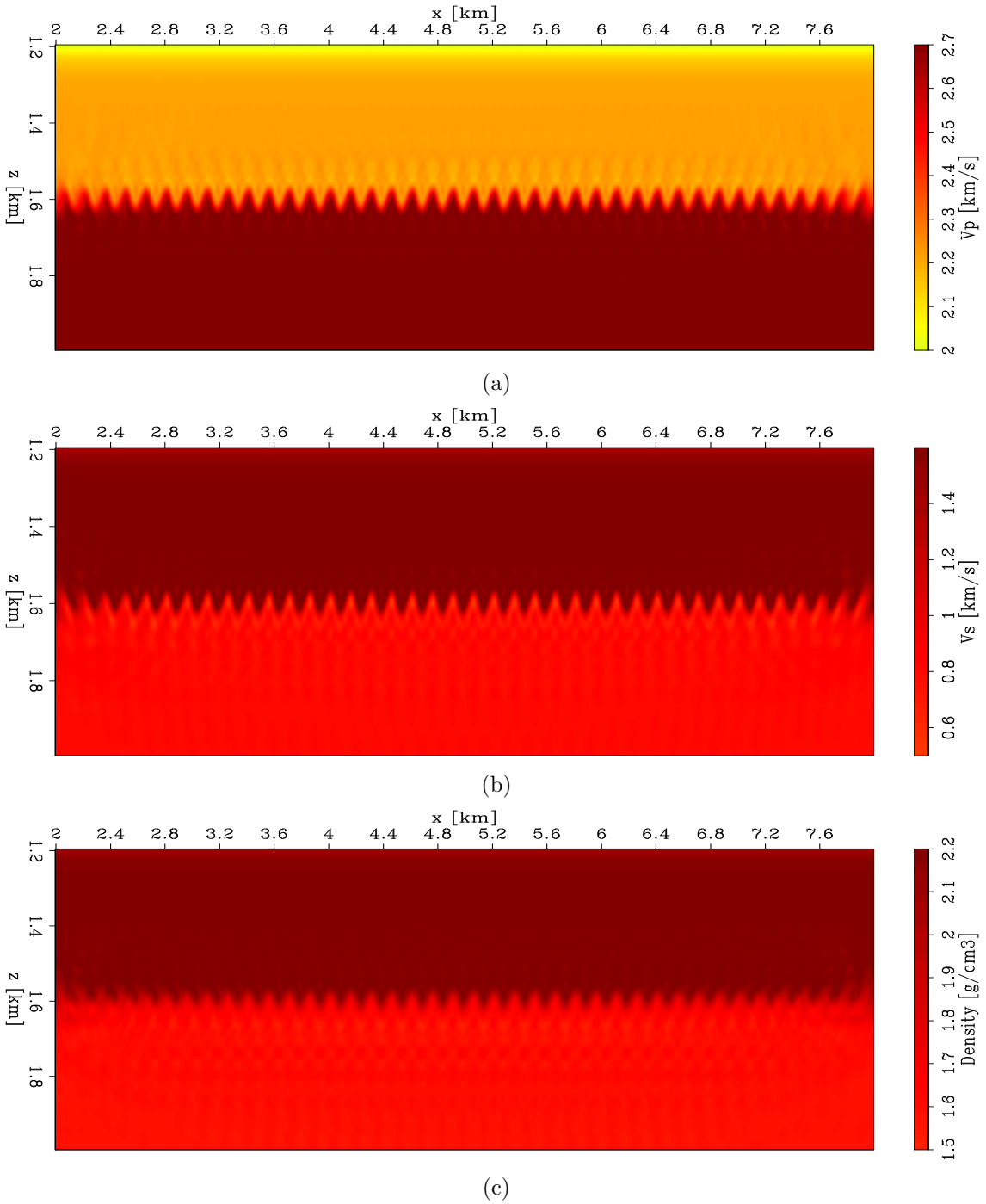

Figure 7: Elastic FWI result when the correct sunk-acquisition pressure data are inverted. The panels show the inverted parameters: (a) P-wave velocity, (b) S-wave velocity, and (c) density. [**CR**]

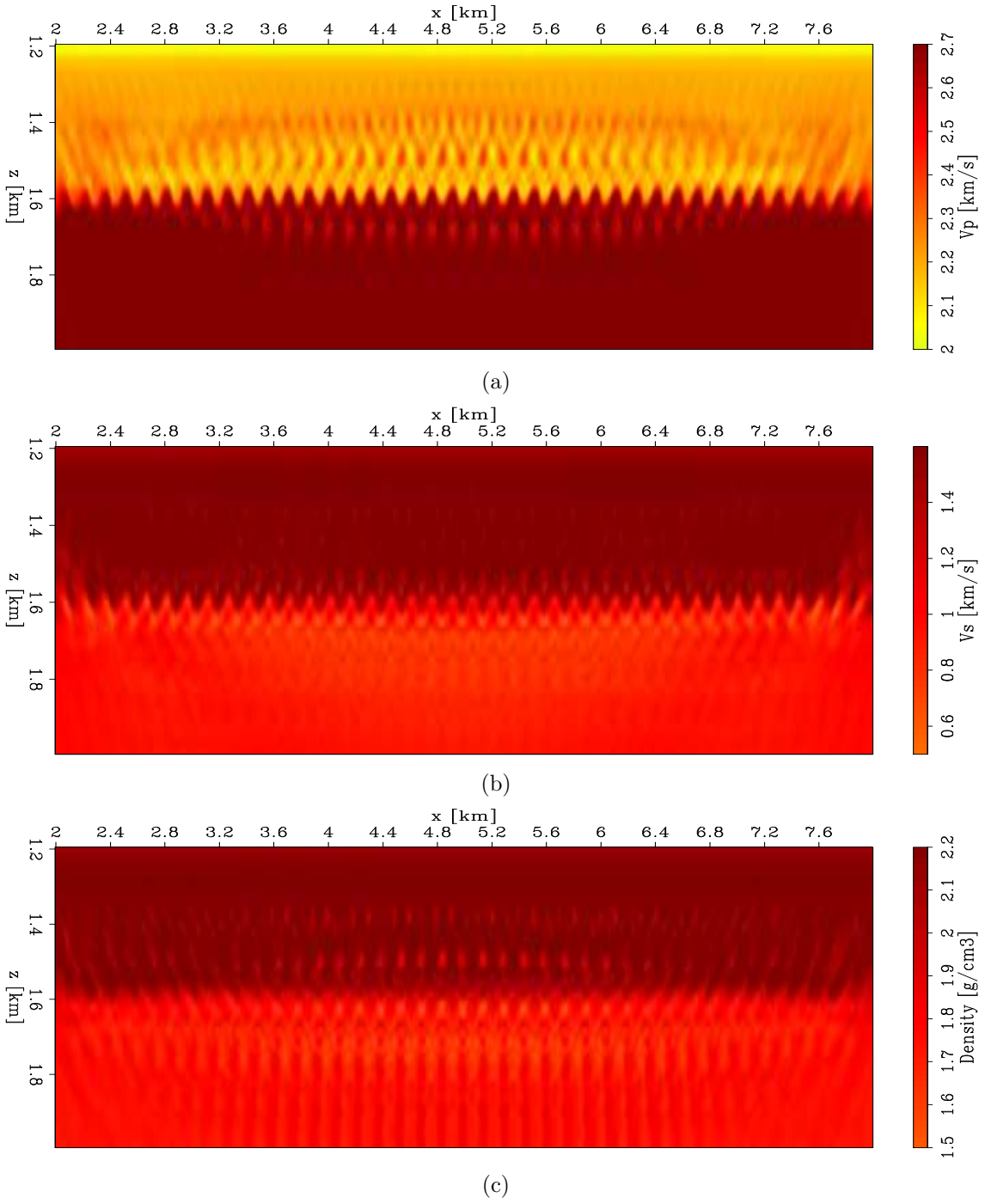

Figure 8: Elastic FWI result when the reconstructed sunk-acquisition pressure data are inverted. The panels show the inverted parameters: (a) P-wave velocity, (b) S-wave velocity, and (c) density. The artifacts present in the inverted parameters are due to the truncation of the linear inversion and to the slightly different illumination between the surface- and sunk-acquisition geometries. [**CR**]

Aster, R., B. Borchers, and C. Thurber, 2005, Parameter Estimation and Inverse Problems: Elsevier.

Bevc, D., 1997, Imaging complex structures with semirecursive kirchhoff migration: Geophysics, **62**, 577–588.

Bozdağ, E., J. Trampert, and J. Tromp, 2011, Misfit functions for full waveform inversion based on instantaneous phase and envelope measurements: Geophysical Journal International, **185**, 845–870.

Bunks, C., F. M. Saleck, S. Zaleski, and G. Chavent, 1995, Multiscale seismic waveform inversion: Geophysics, **60**, 1457–1473.

Claerbout, J. F. and S. M. Doherty, 1972, Downward continuation of moveout-corrected seismograms: Geophysics, **37**, 741–768.

Fichtner, A., 2010, Full seismic waveform modelling and inversion: Springer Science & Business Media.

Hobro, J. W., C. H. Chapman, and J. O. Robertsson, 2014, A method for correcting acoustic finite-difference amplitudes for elastic effects: Geophysics, **79**, T243–T255.

Prucha, M. L., B. L. Biondi, W. W. Symes, et al., 1999, Angle-domain common image gathers by wave-equation migration: Presented at the 1999 SEG Annual Meeting.

Sava, P. C. and S. Fomel, 2003, Angle-domain common-image gathers by wavefield continuation methods: Geophysics, **68**, 1065–1074.

Sirgue, L., O. Barkved, J. Dellinger, J. Etgen, U. Albertin, and J. Kommedal, 2010, Thematic set: Full waveform inversion: The next leap forward in imaging at Valhall: First Break, **28**, 65–70.

Tarantola, A., 1984, Inversion of seismic reflection data in the acoustic approximation: Geophysics, **49**, 1259–1266.

Veitch, B., J. Rickett, and J. Hobro, 2012, Imaging elastic media by corrections to acoustic propagation: Presented at the 2012 SEG Annual Meeting.

Virieux, J., 1986, P-SV wave propagation in heterogeneous media: Velocity-stress finite-difference method: Geophysics, **51**, 889–901.

Virieux, J. and S. Operto, 2009, An overview of full-waveform inversion in exploration geophysics: Geophysics, **74**, WCC1–WCC26.

Wapenaar, C., H. Cox, and A. Berkhout, 1992, Elastic redatuming of multicomponent seismic data: Geophysical prospecting, **40**, 465–482.

Yilmaz, Ö., 2001, Seismic data analysis, volume **1**: Society of Exploration Geophysicists Tulsa.